Two Photon Physics at Future Linear Colliders

A. De Roeck*

* *CERN 1211 Geneva 23 Switzerland*
e-mail: deroeck@mail.cern.ch

Abstract. Prospects for QCD studies in two-photon interactions at a future linear e^+e^- and $\gamma\gamma$ collider are discussed.

I INTRODUCTION

Traditionally e^+e^- colliders provide a wealth of two-photon data. The photons are produced via bremsstrahlung [1] from the electron and positron beam, which leads to a soft energy spectrum for the photons. Such processes will also occur at future high energy (0.5-1 TeV) e^+e^- colliders, but due to the "single time" usage of the colliding beams these will allow other operation modes, such as a photon collider mode. A photon collider [2,3], where the electron beams of a linear e^+e^- collider are converted into photon beams via Compton laser backscattering, offers an exciting possibility to study two-photon interactions at the highest possible energies, with high luminosity. A plethora of QCD physics topics in two-photon interactions can be addressed with a linear e^+e^- collider or photon collider. In this mini review we discuss perspectives for measurements of the total cross-section, the photon structure function and the onset of large logarithms in the QCD evolution.

II TOTAL CROSS SECTION

The total $\gamma\gamma$ cross-section is not yet understood from first principles. Fig. 1 shows the present photon-photon cross-sections data in comparison with recent phenomenological models [4]. All models predict a rise of the cross-section with the collision energy, $\sqrt{s}_{\gamma\gamma}$, but the amount of the rise differs and predictions for high photon-photon energies show dramatic differences. In *proton-like-models* (dash-dotted [5,6], dashed [8],dotted [9] and solid [10] curves), the curvature follows closely that of proton-proton cross-section, while in *QCD based* models (upper [7] and lower [4,6] bands), the rise is obtained using the eikonalized PQCD jet cross-section.

The figure demonstrates that large differences between the models become apparent in the energy range of a future 0.5-1 TeV e^+e^- collider. A detailed comparison of the predictions [4] reveals that in order to distinguish between all the models the cross-sections need to be determined to a precision of better than 10%. This is difficult to achieve in the e^+e^- collider mode, since the variable $\sqrt{s}_{\gamma\gamma}$ needs to be reconstructed from the visible hadronic final state in the detector. At the highest energies, the hadronic final state extends in pseudorapidity $\eta = \ln\tan\theta/2$ in the region $-8 < \eta < 8$, while the detector covers roughly the region $-3 < \eta < 3$. However, for a photon collider the photon beam energy can be tuned with a spread of less than 10%, such that measurements of $\sigma^{tot}_{\gamma\gamma}$ can be made at a number of different energy values in the range $50 < \sqrt{s}_{\gamma\gamma} < 400$ GeV. The absolute precision with which these cross-sections can be measured ranges from 5% to 10%, where the largest contributions to the errors are due to the control of the diffractive component of the cross-section, Monte Carlo models used to correct for the event selections, the absolute luminosity and knowledge on the shape of the luminosity spectrum. It will be necessary to constrain the diffractive component in high energy two-photon data. A technique to measure diffractive contributions separately, mirrored to the rapidity gap methods used at HERA, has been proposed in [11].

III PHOTON STRUCTURE

The nature of the photon is complex. A high energy photon can fluctuate into a fermion pair or even into a bound state, i.e. a vector meson with the same quantum numbers as the photon $J^{PC} = 1^{--}$. These quantum fluctuations lead to the so-called hadronic structure of the photon. In contrast to the structure function of the proton the structure function of the photon is predicted to rise linearly with the logarithm of the momentum transfer Q^2, and to increase with increasing Bjorken-x [12]. The absolute magnitude of the photon structure function is asymptotically determined by the strong coupling constant [13].

The classical way to study the structure of the photon is via deep inelastic electron-photon scattering, i.e. two-photon interactions with one quasi-real (virtuality $Q^2 \sim 0$) and one virtual ($Q^2 >$ few GeV^2) photon. The unpolarised $e\gamma$ DIS cross-section is

$$\frac{d\sigma(e\gamma \to eX)}{dQ^2dx} \;=\; \frac{2\pi\alpha^2}{Q^4x} \cdot \left[\{1+(1-y)^2\}F_2^\gamma(x,Q^2) - y^2F_L^\gamma(x,Q^2)\right], \qquad (1)$$

where $F^\gamma_{2,L}(x,Q^2)$ denote the structure functions of the real photon.

To measure F_2^γ it is important to detect (tag) the scattered electron which has emitted the virtual photon. Background studies suggest that these electrons can be detected down to 25 mrad and down to 50 GeV. $e\gamma$ scattering at a photon collider resembles experimentally ep scattering at HERA, i.e. the energy of the probed quasi-real photon is known (within the beam spread of 10%) and the systematic error can be controlled to about 5%. Fig. 2 shows the measurement potential for

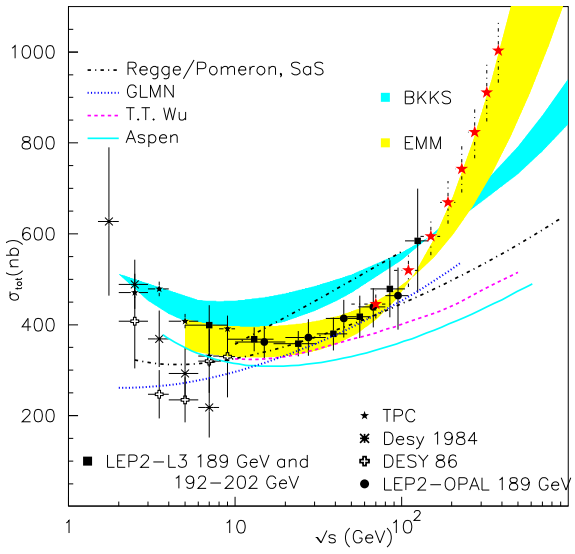

FIGURE 1. The total $\gamma\gamma$ cross-section as function of the $\gamma\gamma$ collision energy, compared with model calculations: BKKS band (upper and lower limit correspond to different photon densities); SAS lines (Regge Pomeron exchange, upper and lower limits as given by SAS); Aspen (QCD inspired model, satisfying factorization); EMM band (Eikonal Minijet Model for total and inelastic cross-section, with different photon densities and different minimum jet transverse momentum).

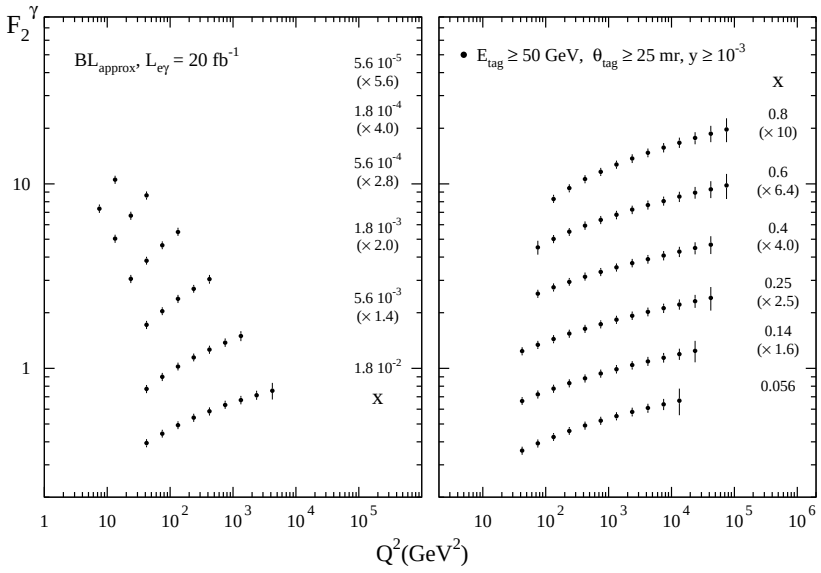

FIGURE 2. The kinematic coverage of the measurement of F_2^γ for the backscattered $e\gamma$ mode at a 500 GeV linear collider.

a photon collider [14]. The measurements are shown with statistical and (5%) systematical error, for 20 fb^{-1} photon collider luminosity, i.e. about a year of data taking. Measurements can be made in the region $5.6 \cdot 10^{-5} < x < 0.56$, i.e. in a region similar to the HERA proton structure function measurements, and $10 < Q^2 < 8 \cdot 10^4$ GeV^2. For the e$^+$e$^-$ collider mode the hadronic final state needs to be measured accurately in order to reconstruct x. This will limit the lowest reachable x value around 10^{-3}. It will enable however measurements in the high x ($0.1 < x < 0.8$) and high Q^2 ($Q^2 > 100$ GeV^2) range, for detailed F_2^γ QCD evolution tests [15].

The Q^2 evolution of the structure function at large x and Q^2 has also been often advocated as a clean measurement of α_s. A 5% change on α_s results however in a 3% change in F_2^γ only, hence such a α_s determination will require very precise F_2^γ measurements.

At high Q^2 values, apart from γ exchange, also Z and W exchange will become important, the latter leading to charged current events [16] which leads to spectacular signals due to the escaping neutrino with high transverse momentum. By measuring the electroweak neutral and charged current structure functions, the up and down type quark content of the photon can be determined separately.

While $e\gamma$ scattering allows to measure the quark distributions it only constrains the gluon distribution via the QCD evolution of the structure functions. Direct information on the gluon in the photon can however be obtained from measurements of jet and charm production [17] in $\gamma\gamma$ collisions at an e$^+$e$^-$ or $\gamma\gamma$ collider. Fig. 3 shows the Di-jet cross-section as function of $x_\gamma = x_\gamma^\pm = \Sigma_{jets}(E \pm p_z)/\Sigma_{hadrons}(E \pm p_z)$, with p_z the longitudinal momentum of a particle. This variable is closely related to the true x_γ at the parton level, and can be used to separate resolved (e.g. $x_\gamma^\pm < 0.8$) from direct (e.g. $x_\gamma^\pm > 0.8$) processes. The x_γ distribution is shown for two different assumptions of the parton distributions in dijet production. x_γ values down to a few times 10^{-3} can be reached with charm and di-jet measurements [18].

A linear collider also provides circularly polarised photon beams, either from the polarised beams of the e$^+$e$^-$ collider directly, or via polarised laser beams scattered on the polarised e$^+$e$^-$ drive beam. This offers a unique opportunity to study the polarised parton distributions of the photon, for which no experimental data are available to date.

Information on the spin structure of the photon can be obtained from inclusive polarised deep inelastic $e\gamma$ measurements and from jet and charm measurements [19,20] in polarised $\gamma\gamma$ scattering. An example of a jet measurement is presented in Fig. 4 which shows the asymmetry measured for dijet events, for the e$^+$e$^-$ and photon collider modes separately. Two extreme models are assumed for the polarised parton distributions in the photon. Already with very modest luminosity significant measurements of the polarised parton distributions become accessible at a linear collider. The extraction of the polarised structure function $g_1(x, Q^2) = \Sigma_q e_q^2(\Delta q^\gamma(x, Q^2) + \Delta\overline{q}^\gamma(x, Q^2))$, with Δq the polarised parton densities, can however be best done at a $e\gamma$ collider. Measurements of g_1, particularly at low x, are extremely important for studies of the high energy QCD limit, or

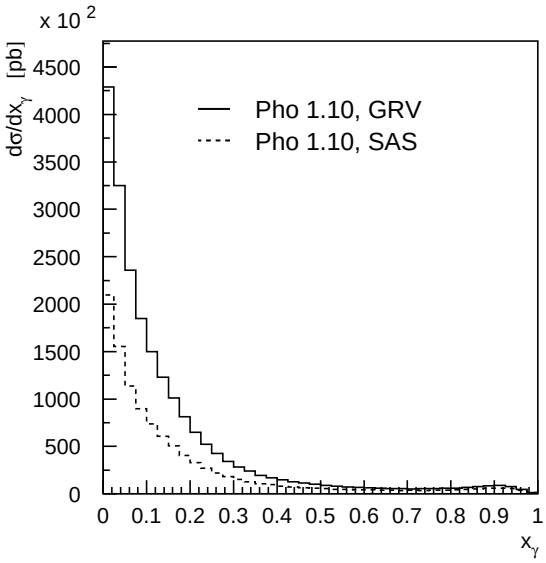

FIGURE 3. Jet cross-sections versus x_γ for the backscattered $\gamma\gamma$ mode at a 500 GeV linear collider, for two assumptions of parton distributions of the photon.

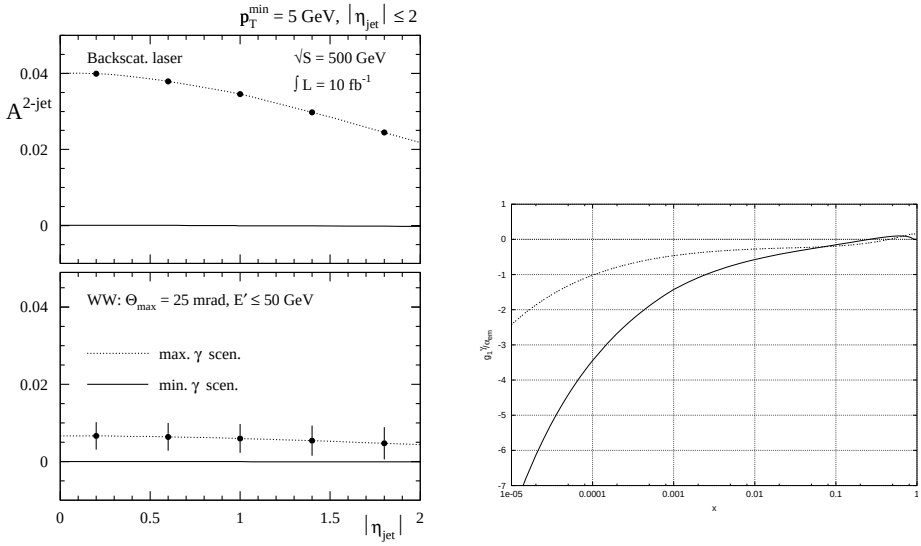

FIGURE 4. (left) di-jet spin asymmetry for events with $x_\gamma^{\pm} < 0.8$, $p_T^{jet} = 5$ GeV and $|\eta_{jet}| < 2$ for $e\gamma$ (top) and $\gamma\gamma$ (bottom) collisions. Predictions are shown for two different assumptions for the polarized parton distributions of the photon. (right) Predictions for g_1 calculated without (dashed line) and with (full line) $\alpha_s^n \ln^{2n} 1/x$ effects.

BFKL regime [21]. Indeed, the most singular terms of the effects of the small x resummation on $g_1(x,Q^2)$ behave like $\alpha_s^n \ln^{2n} 1/x$, compared to $\alpha_s^n \ln^n 1/x$ in the unpolarised case of F_2^γ. Thus large $\ln 1/x$ effects are expected to set in much more rapidly for polarised than for unpolarised structure measurements. Fig. 4 shows that for leading order calculations, including kinematic constraints, the differences in predictions for g_1 with and without these large logarithms can be as large as a factor 3 to 4 for $x = 10^{-4}$ and could thus be easily measured with a few years of data taking at a photon collider.

IV TESTING OF BFKL DYNAMICS

Apart from the inclusive polarised structure function measurements, discussed in the previous section, several dedicated measurements exist for detecting and studying the large $\ln 1/x$ logarithm resumation effects in QCD, also called BFKL dynamics.

The most promising measurement for observing the effect of the large logarithms is the total $\gamma^*\gamma^*$ cross-section, i.e. two-photon scattering of virtual photons with approximately equal virtualities for the two photons. Recent calculations, taking into account higher order effects, confirm that this remains a gold-plated measurement, which can be calculated essentially entirely perturbatively and has a sufficiently large cross-section. The events are measured by tagging both scattered electrons. At a 500 GeV e^+e^- collider about 3000 events are expected per year (200 fb^{-1}) and a factor of 3 less in the absence of BFKL effects in the data [23]. Tagging electrons down to as low angles as possible (e.g. 25 mrad) is however a crucial requirement for the experiment. The growth of the cross section as function of W^2 due to the BFKL effect is shown in Fig.5, (solid line) and compared with the cross section in absence of BFKL (dashed line).

Closely related to the $\gamma^*\gamma^*$ measurement is vector meson production, e.g $\gamma\gamma \to J/\psi J/\psi$ or (at large t) $\gamma\gamma \to \rho\rho$, where the hard scale in the process is given by the J/ψ mass or the momentum transfer t. J/ψ's can be detected via their decay into leptons, and separated from the background through a peak in the invariant mass. Approximately 100 fully reconstructed 4-muon events are expected for 200 fb^{-1} of luminosity for a 500 GeV e^+e^- collider [24]. For this channel it is crucial that the decay muons and/or electrons can be measured to angles below 10 degrees in the experiment.

A process similar to the 'forward jets' at HERA can be studied at a linear collider in $e\gamma$ scattering, with a forward jet produced in the direction of the real photon. The measurements can reach out to smaller x values than presently reachable at HERA, due to the more favourable kinematics of the final state [25].

Finally the processes $e^+e^- \to e^+e^-\gamma X$ and $\gamma\gamma \to \gamma X$ have been studied [26], and found to be very sensitive to BFKL dynamics. Event rates for events with photons with energy larger than 5 GeV and p_T larger than 1 GeV are large. At an e^+e^- collider several thousand events will be collected per year, while at a photon

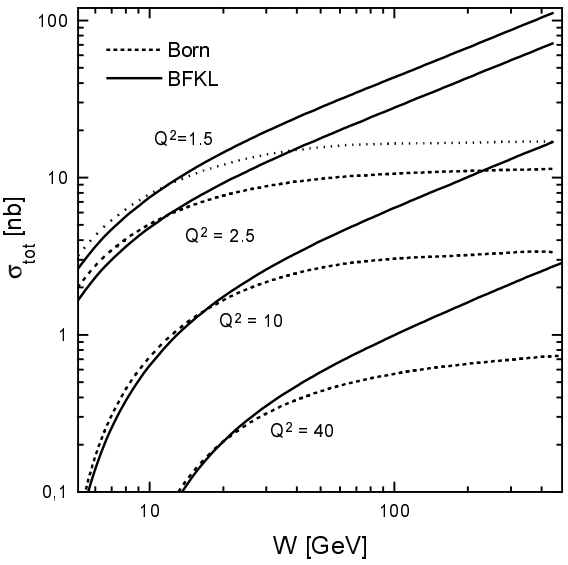

FIGURE 5. Prediction of the $\sigma_{\gamma^*\gamma^*}(Q^2, Q^2, W^2)$ cross section (solid line) and two gluon exchange cross section (dotted line) as function of W^2 for different Q^2 values.

collider the event rate is about a factor ten larger.

In all, the study of these processes will provide new fundamental insight in small x QCD physics.

V CONCLUSION

Future linear e^+e^- and $\gamma\gamma$ colliders offer a great opportunity to study photon interactions and QCD processes in detail.

REFERENCES

1. C. F. Weizsäcker, Z. Phys. **88** (1934) 612; E.J. Williams, Phys. Rev. **45** (1934)729.
2. I.F.Ginzburg, G.L.Kotkin, V.G.Serbo and V.I.Telnov, Nucl. Instr. and Meth. **205** (1983) 47; I.F.Ginzburg, G.L.Kotkin, S.L.Panfil, V.G.Serbo and V.I.Telnov, Nucl. Instr. and Meth. **219** (1984) 5.
3. V.I.Telnov, Nucl. Instr. and Meth. **A294** (1990) 72.
4. R.M. Godbole and G. Pancheri, LC-TH note in preparation.
5. G. Schuler and T. Sjostrand, Zeit. Phys. **C68** (1995) 607
6. A. Corsetti, R.M. Godbole and G. Pancheri, Phys. Lett. **B435** (1998) 441, hep-ph/9807236
7. B. Badelek, M. Krawczyk, J. Kwiecinski and M. Stasto, hep-ph/0001161.
8. T.T. Wu, Mod. Phys. Lett. **A15** (2000) 9.

9. E. Gotsman, E. Levin, U. Maor, E. Naftali, Eur.Phys. J. **C14** (2000) 5, hep-ph/0001080.
10. M. Block, E. Gregores, F. Halzen and G. Pancheri, Phys. Rev. **D60** (1999) 54024.
11. A. De Roeck, R. Engel and A. Rostovtsev, hep-ph/9710366.
12. T.F. Walsh and P.M. Zerwas, Phys. Lett., **B44** (1973) 196.
13. E. Witten, Nucl. Phys. **B120** (1977) 189.
14. A. Vogt, Nucl. Phys. Proc. Suppl. **82** (2000) 394;
    A. De Roeck, Proc. of the International Workshop on Linear Colliders (LCWS99) Sitges, May 1999; LC-TH note in preparation
15. R. Nisius, Phys. Rep. **332** (2000) 165.
16. A. Gehrmann-De Ridder, H. Spiesberger, P.M. Zerwas, Phys. Lett. **B469** (1999) 259.
17. P. Jankovski, M. Krawczyk, and A. De Roeck, LC-TH-2000-034, hep-ph/0002169.
18. T. Wengler, A. De Roeck, Proc. of the Workshop on Photon Colliders, DESY, Hamburg, June 2000.
19. M. Stratmann, Nucl. Phys. Proc. Suppl. **82** (2000) 400.
20. J. Kwiecinski and B. Ziaja, hep-ph/0006292.
21. E.A. Kuraev, L.N. Lipatov, V.S. Fadin, Sov. Phys. JETP **45** (1972) 199;
    Y.Y. Balitsky, L.N. Lipatov, Sov. J. Nucl. Phys. **28** (1978) 822.
22. J. Bartels, A. De Roeck and H. Lotter, Phys. Lett. **B389** (1996) 742;
    S. J. Brodsky, F. Hautmann and D.E. Soper, Phys. Rev. **D56** (1997) 6957;
    M. Boonekamp et al., Nucl.Phys. **B555** (1999) 540.
23. J.Kwiecinski, L.Motyka, Phys. Lett. **B462** (1999) 203.
24. J.Kwiencinski, L.Motyka, A. De Roeck, LC-TH-2000-012, hep-ph/0001180.
25. G. Contreras and A. De Roeck, LC-TH note in preparation.
26. N.Evanson and J.Forshaw, LC-TH-2000-010, hep-ph/9912487.